

F.L. Bonali, C. Corazzato, F. Bellotti and G. Groppelli

Abstract

The aim of this review is to describe the state-of-art of the neotectonic setting of this area as well as to present new data resulting from a recent structural field survey. The integrated analysis of literature and new structural data shows incongruities mainly in some regional structures and in the ENE-WSW striking fault system that affects and controls the feeding system of Copahue volcano. In addition, taking into account the very recent volcanic activity, the structural constraints and the earthquakes occurred in the area close to the volcano, a static stress numerical model was applied to simulate the variations of the local stress perturbing the normal activity of the volcanic plumbing system favouring magma ascent and consequent eruptions. At present, a comprehensive structural model is lacking and more in-depth studies can furnish a complete tectonic framework of the area, which can provide fundamental information to assess volcanic hazard, forecast future volcanic activity, and to enhance the development of the associated geothermal field.

F.L. Bonali · C. Corazzato
Dipartimento di Scienze dell'Ambiente e del
Territorio e di Scienze della Terra, Università di
Milano-Bicocca, Piazza della Scienza 4, 20126
Milan, Italy

C. Corazzato
Dipartimento di Scienza e Alta Tecnologia,
Università dell'Insubria, Como, Italy

F. Bellotti
Tele-Rilevamento Europa T.R.E. s.r.l, Ripa di Porta
Ticinese 79, 21149 Milan, Italy

G. Groppelli (✉)
Istituto per la Dinamica dei Processi Ambientali—
Sezione di Milano, Consiglio Nazionale delle
Ricerche, via Mangiagalli 34, 20133 Milan, Italy
e-mail: gianluca.groppelli@cnr.it

2.1 Introduction

Active tectonics is capable of influencing activity at volcanoes both at local and regional scale, controlling the feeding system geometry, the magma rising, and the growth-dismantlement phases of volcanic edifices (Marzocchi et al. 1993; Barrientos 1994; Decker et al. 1995; Bautista et al. 1996; Nostro et al. 1998; Bellotti et al. 2006; Walter and Amelung 2006; Norini et al. 2008, 2010, 2013; Groppelli and Norini 2011; Bonali et al. 2013; Bonali 2013). Active tectonics also impacts the hydrothermal circulation and consequently geothermal fields in volcanic areas,

by developing faults and fractures in the upper crust (e.g. Cameli et al. 1993; Brogi et al. 2010; Giordano et al. 2013; Norini et al. 2013).

The purpose of this chapter is to present the state of the art on Copahue volcano, an active Andean volcano located in the eastern Andean Southern Volcanic Zone, where a close connection between tectonic control, volcanic activity and the associated geothermal field is well documented in previous works (e.g. Velez et al. 2011, and references therein). The resolution of the neotectonic setting around Copahue volcano has been improved in this chapter by means of a detailed structural field survey performed in 2007, mainly devoted to recognising the evidence of active tectonics and the relationship among the fault pattern, the volcanic feeding system and the eruptive history.

Moreover, for the reason that large earthquakes could trigger volcanic activity at both close and large distances from the epicentre at regional scale (Linde and Sacks 1998; Hill et al. 2002; Marzocchi 2002a, b; Marzocchi et al. 2002; Manga and Brodsky 2006; Walter and Amelung 2007; Eggert and Walter 2009; Bebbington and Marzocchi 2011) in a time-frame of a few days after the earthquake event (Linde and Sacks 1998; Manga and Brodsky 2006; Eggert and Walter 2009; Moreno and Petit-Breuilh 1999), a static stress numerical model was also applied to simulate the variations in the local stress induced by earthquakes on the plumbing system.

Structural data in combination with numerical modelling can provide fundamental information to forecast future volcanic activity and to assess volcanic hazard. Finally, the in-depth knowledge of the tectonic setting of Copahue volcano can enhance the development and exploitation of the geothermal field, because of the structural control on hydrothermal circulation (Giordano et al. 2013; Invernizzi et al. 2014).

2.2 Volcanotectonic Setting

As highlighted by Folguera et al. (2015), the 2997 m-high Copahue active stratovolcano is located in the eastern part of the Southern

Volcanic Zone (SVZ) (Fig. 2.1). The deformation in the study area is partitioned in such a way that large thrust earthquakes dominantly occur in the subduction zone, whereas intra-arc transcurrent faulting events are observed (Barrientos and Ward 1990; Cisternas et al. 2005; Watt et al. 2009). Dextral strike-slip moment tensor solutions dominate between 34° and 46°S in the main cordillera (e.g. Chinn and Isacks 1983; Lange et al. 2008), although it is only south of 38°S that long-term strike-slip faulting shows surface evidence, represented by the 1200 km-long Liquiñe-Ofqui major intra-arc fault zone (LOFZ, Figs. 2.1 and 2.2; Cembrano et al. 1996; Folguera et al. 2002; Adriasola et al. 2006; Rosenau et al. 2006; Cembrano and Lara 2009). This dextral transpressional fault zone plays a fundamental role in controlling the magmatic activity along the volcanic front between 37° and 47°S (Lavenu and Cembrano 1999; Rosenau 2004). López-Escobar et al. (1995) and Cembrano and Lara (2009) suggested that, with respect to the more contractional setting further north in the SVZ, the LOFZ allows a more rapid magma ascent with lesser occurrence of crustal assimilation or magma mixing (Collini et al. 2013). Folguera et al. (2006, 2015) recognise a transition from the strike-slip fault zone to a thrust zone at approximately 37°S, testified by the merging of the LOFZ into the Agrio and the Malargue fold-and-thrust belts (Fig. 2.1). This transition also corresponds to a thickening and ageing of the continental crust (Rojas Vera et al. 2014), to longer crustal magma residence times, and to greater differentiation, crustal assimilation and magma mixing (Tormey et al. 1991).

The name “Caviahue-Agrio caldera”, where Copahue volcano is located (Figs. 2.2a and 2.3), encompasses both names that this structure was given in the literature, Caviahue caldera (Melnick et al. 2006; Velez et al. 2011) and Agrio caldera (Melnick and Folguera 2001; Rosenau et al. 2006; Rojas Vera et al. 2009) respectively. It is described as a pull-apart basin, a transtensional structural system developed in the north-eastern end of the LOFZ by dextral movements in the late Pliocene (Melnick and Folguera 2001;

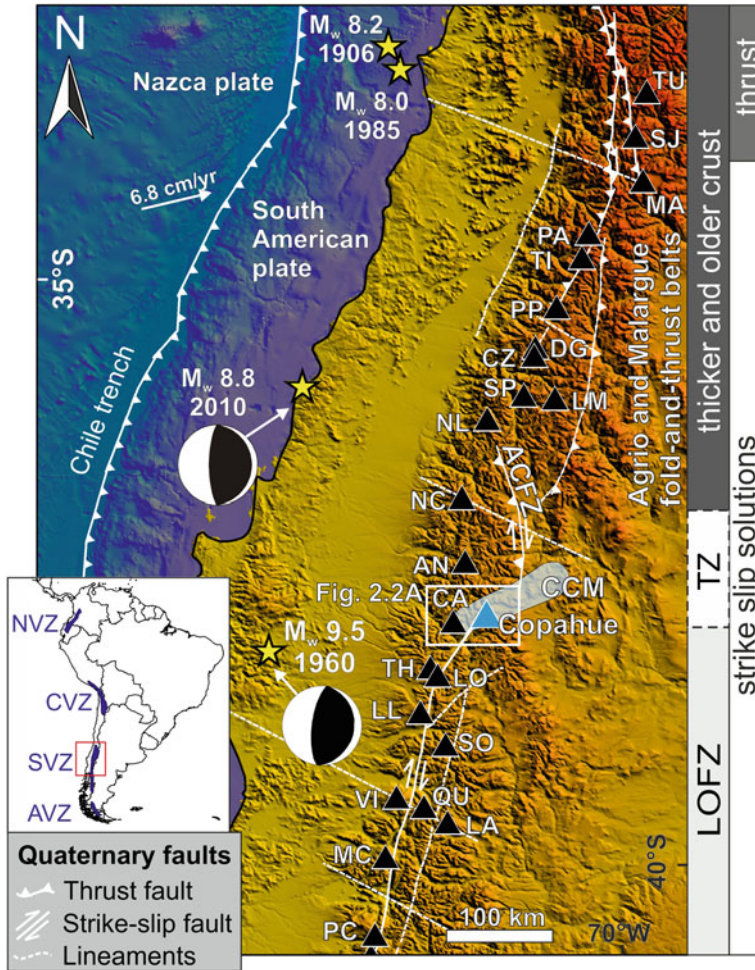


Fig. 2.1 Tectonic setting of the Southern Volcanic Zone (SVZ). Triangles locate active Holocene volcanoes. The white arrow indicates the approximate convergence direction of the plates with estimated velocity. Main intra-arc faults with reverse motion (thrust faults) in the north, and right lateral strike-slip motion in the south are reported (redrawn after Melnick et al. 2006; Cembrano and Lara 2009; Bonali 2013). LOFZ-Liquiñe-Ofqui Fault Zone; TZ-Transition Zone; CCM-Callaqui-Copahue-Mandolegüe lineament, ACFZ-Antinir-Copahue regional thrust-fold system. NVZ, CVZ, SVZ and AVZ correspond

to Northern, Central, Southern and Austral Volcanic Zones. TU-Tupungatito; SJ-San José; MA-Maipo; PA-Palomo; TI-Tinguiririca; PP-Planchón-Peteroa; DG-Descabezado Grande; CZ-Cerro Azul; NL-Nevado de Longavi, NC-Nevados de Chillán; AN-Antuco; CA-Callaqui; TH-Tolhuaca; LO-Lonquimay; LL-Llaima; VI-Villarrica; QU-Quetrupillan; LA-Lanin; MC-Mocho-Choshuenco; PC-Puyehue-Cordón Caulle. Yellow stars locate earthquakes with $M_w \geq 8$ occurred since 1900 AD, focal mechanisms of the modelled earthquakes are reported

Folguera et al. 2015) and part of the abovementioned transition zone between the Andean segments to the north and south (Lavenu and Cembrano 1999). The LOFZ shows clear evidence of Plio-Quaternary dextral kinematics, and the main active fault of this area is the

NE-striking Lomin fault (LF in Fig. 2.2), ending at the southwestern border of the Caviahue-Agrio caldera and representing the most relevant expression of a horsetail-like array and affecting Holocene lavas of Copahue volcano (Melnick 2000; Melnick et al. 2006).

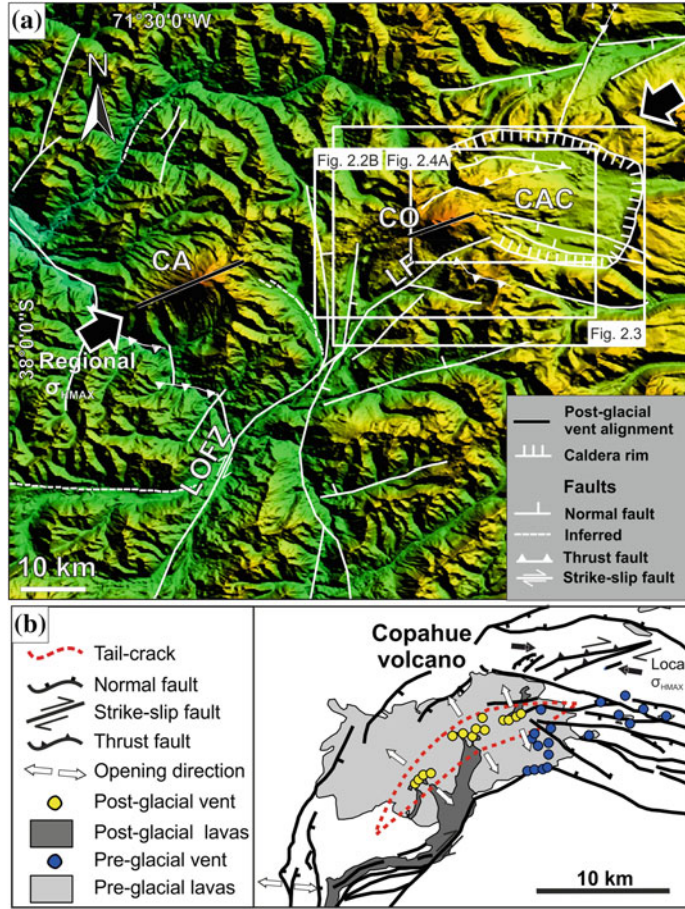


Fig. 2.2 a Tectonic map of the Callaqui-Copahue-Mandolegüe transfer zone (CCM). CAC Caviahue-Agrio Caldera; LOFZ Liquiñe-Ofqui fault zone; LF Lomin fault; CA Callaqui volcano; CO Copahue volcano. *Thick black lines* represent the strike of volcano feeding systems, while *black arrows* represent the regional σ_{Hmax} .

Shaded-relief digital elevation model is from SRTM90 data (datum WGS84) (<http://srtm.csi.cgiar.org/>). Boxes locate Figs. 2.2b, 2.3 and 2.4a. **b** Structural model of the Copahue volcanic complex characterized by a N60 °E trending post-glacial vent alignment. Redrawn from Melnick et al. (2006)

2.3 Active Tectonics – Literature Data

Several authors described the tectonics of the Caviahue-Agrio caldera—Copahue volcano complex, further on named as CAC as in Melnick et al. (2006), while in Velez et al. (2011) it is reported as CCVC (Caviahue caldera—Copahue stratovolcano). A recent structural synthesis is provided by Folguera et al. (2015) and references therein. Here, the focus is on the evidence of active tectonics in the CAC area as reported in

the literature, and further original field data are provided to understand the tectonic structures presently controlling the volcanic activity of Copahue and the geothermal resources of the area.

The CAC represents an arc volcanic complex in an oblique subduction setting, and it is located in an important morphotectonic zone, transitional from strike-slip to thrust-dominated (Melnick et al. 2006). It represents the central sector of the NE-trending, 90-km-long Callaqui-Copahue-Mandolegüe (CCM) volcanic alignment (Fig. 2.1), the longest Plio–

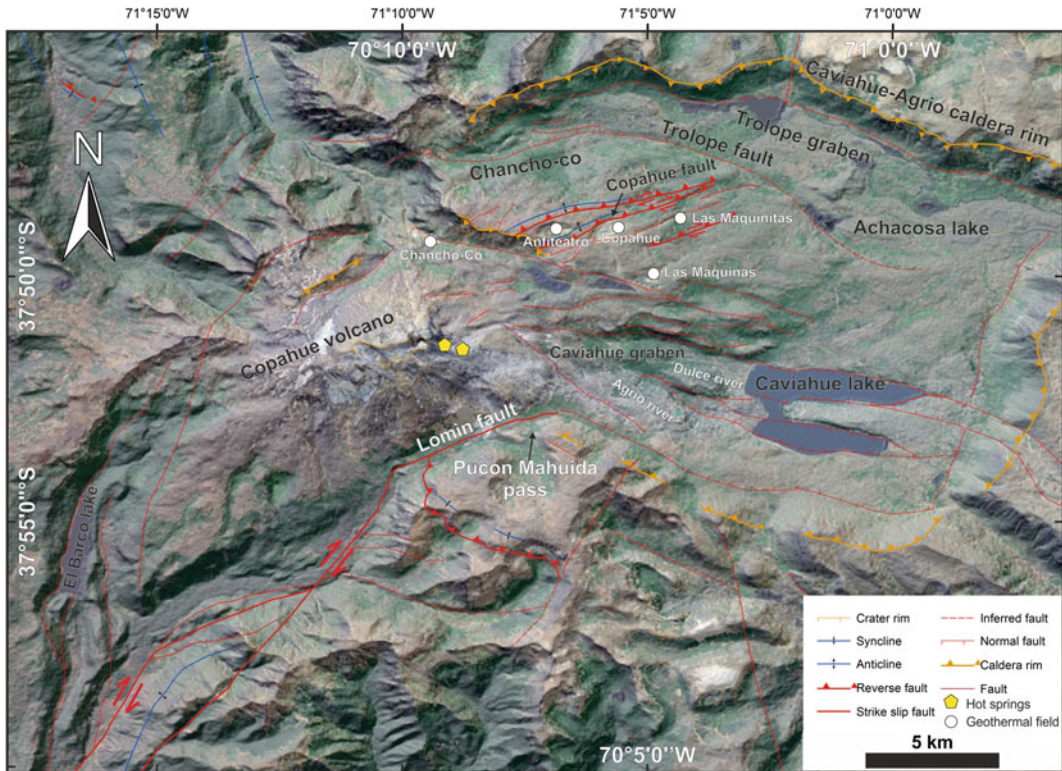


Fig. 2.3 Main structural features of the Caviahue-Copahue complex mapped on Aster DTM and Image (redrawn from Melnick et al. 2006). Geothermal fields are indicated after Velez et al. (2011)

Quaternary volcanic alignment of the SVZ (Melnick et al. 2006) and regarded as a transfer zone accommodating the step-wise configuration of the strike-slip LOFZ, controlled at the arc front, and the Antinir-Copahue regional thrust-fold system (ACFZ in Fig. 2.1, as defined in Folguera et al. 2004; Folguera and Ramos 2009; Velez et al. 2011, also named CAFS in Melnick et al. 2006), running through the inner retroarc (Melnick and Folguera 2001; Radic et al. 2002; Folguera et al. 2004; Melnick et al. 2006), with persistent activity in the Holocene. Melnick and Folguera (2001) described the Quaternary volcano-tectonic phase of activity of the area as mixed transtensional and transpressive, in close spatial relation with the CCM volcanic alignment. The following subsections describe in detail the state of the art on the active structures in the CAC, in particular the Caviahue-Agrío caldera, the structures located

south of Copahue volcano, the WNW-striking system, the Chancho-Co structures, and the Copahue Fault.

2.3.1 The Caviahue-Agrío Caldera

The Caviahue-Agrío caldera (Figs. 2.2 and 2.3), 15-km-long and 10-km-wide, formed as a volcanic feature with a strong structural control. Volcanic activity in the Caviahue-Agrío caldera area has been controlled by both the regional stress field imposed by plate convergence and by local structures formed at the intersection of regional fault systems (Melnick et al. 2006). The main structures of the Caviahue-Agrío caldera area are represented by (1) the normal faults of the caldera border, building up-to-400-m high scarps affecting Lower Pliocene units, (2) the right-lateral strike-slip faults affecting Copahue postglacial lava flows in the Lomín valley to the

south of the volcano, (3) the NE-trending fissure system controlling the effusive products of Copahue volcano and the hydrothermal manifestations inside the caldera, and (4) the NE-trending imbricated Chancho-Co fault system (Folguera and Ramos 2000, Mazzoni and Licitra 2000), (5) the WNW-trending Caviahue graben, hosting the Agrio lake, and (6) the NE-striking reverse fault affecting the Cola de Zorro formation to the south of the volcano (Melnick and Folguera 2001). Deflation processes at the intersection between the Caviahue graben and the Chancho-Co antiform have been recently recognized by radar interferometry (Ibáñez et al. 2008). Moreover, the CAC area includes several active geothermal fields, showing manifestations of boiling pools and bubbling pools (Velez et al. 2011), namely Las Máquinas, Maquinitas, Copahue, Anfiteatro and Chancho-Co (Fig. 2.3), which are aligned through the Chancho-Co frontal structures (Varekamp et al. 2001; Velez et al. 2011).

In the northern and central part of the Caviahue-Agrio caldera, Folguera et al. (2004) and Rojas Vera et al. (2009) recognise reverse faults with subordinate right-lateral components, affecting post-glacial products and displacing Quaternary morphologies, and producing small pull-apart basins. These structures are associated with the ENE-trending Mandolegue fault system, which represents a transfer zone between the LOFZ and the ACFZ, and whose western edge is represented by the Chancho-Co uplift. Based on fault activity in unconsolidated deposits, Folguera et al. (2004) suggests ongoing deformation for the ACFZ, an E-vergent arrangement of high-angle dextral transpressive and transtensive faults.

2.3.2 The Structures South of Copahue

To the south of Copahue and SW of the Caviahue-Agrio caldera, the NNE-striking Lomín Fault corresponding to the northern edge of the LOFZ, is another Quaternary-active strike slip structure with minor normal component (LF in Figs. 2.2 and 2.3; Folguera et al. 2004), for

which Melnick et al. (2000) and Melnick et al. (2006) recognise neotectonic activity evidenced by 300–1000 m long and up to 5–10 m high fault scarps cutting Holocene lavas erupted from the volcano, close to the Pucón-Mahuida Pass (Fig. 2.3). An at least Pleistocene activity is recognized for the NE-striking structures affecting the southern flank of Copahue (Rojas Vera et al. 2009).

2.3.3 WNW-Striking Structures and Grabens

The WNW-striking normal fault system affects the eastern and central, as well as the northern and southern sectors of the caldera, cutting the Las Mellizas sequence and andesites from the base of Copahue volcano (Fig. 2.3). These faults have a strong topographic expression, and from N to S they form the Trolope and Caviahue grabens, controlling the elongated shape of Lake Caviahue (Melnick et al. 2006). The general strike of the Trolope and Caviahue grabens is parallel to the long axis of the rectangular Caviahue-Agrio caldera, and their formation is related to late Pliocene-Pleistocene reactivation of the caldera-pull-apart structure in response to dextral shear along the LOFZ (Melnick et al. 2006). The Quaternary extensional activity of these grabens represents the latest pulse of the caldera activity, and the Caviahue graben reveals a differential amount of extension from Copahue volcano to the east (Folguera et al. 2004). The Trolope graben affects the Las Mellizas formation, and its most recent control is over singlacial monogenetic cones (Rojas Vera et al. 2009). Copahue volcano is located at the intersection between two main structural systems, the WNW-trending Caviahue graben and the NE-trending Chancho-Co antiform (cfr. 2.3.4), the second main positive feature in the area (Fig. 2.3).

2.3.4 The Chancho-Co Structure

The Chancho-Co structure (Fig. 2.3) is located in the central to northern part of the CAC and is

considered to have been active during the Pleistocene and Holocene, controlling the main active geothermal systems in the area that form an en-echélon arrangement (Melnick et al. 2006). The Chancho-Co is a N60 °E trending elongated ridge (Folguera et al. 2004), representing a transpressive imbricated structure whose development is linked to a series of SE-vergent NE-trending thrusts and associated hanging-wall anticlines (Folguera and Ramos 2000), affecting Late Pliocene successions gathered in Las Mellizas Formation (Melnick et al. 2006). Its uplift would have preceded the extension that led to the Cavihue graben formation (Rojas Vera et al. 2009), and its front is in correspondence of the inhabited Copahue village. There is poor evidence of the potential Quaternary activity of these structures and of their relations with Copahue volcano, or of their deep control (Rojas Vera et al. 2009). The control on the Quaternary and present uplift of the Chancho-Co structure is exerted by a main NE-striking fault system and a subordinate WNW-striking system, coinciding with the geometry of the southernmost part of a gravimetric low (Rojas Vera et al. 2009).

Regarding neotectonic activity along this structure, several authors noticed that: (i) some reverse scarps, a few metres high, affect a glacial surface, together with open cracks (Folguera and Ramos 2000; Folguera et al. 2004); (ii) the southernmost of these reverse faults (defined as the “Copahue Fault” by Rojas Vera et al. 2009, cfr. 2.3.5 and Fig. 2.3) marks the main topographic break, thrusting ignimbrites over Quaternary till-like deposits near the Copahue village (Melnick et al. 2006); (iii) Rojas Vera et al. (2009) describe south-facing reverse fault scarps that uplift the Chancho-Co antiform and affect less than 1 Ma-old volcanics and postglacial Copahue products, as well as Pleistocene glacial morphologies; (iv) extensional faults and open cracks (extended for tens of meters and reaching depths of 15 m) along the axis of the Chancho-Co anticlines, with scarps up to 3-m high, were described by Melnick et al. (2006). They define small crestal grabens that trend slightly oblique to the reverse faults and the axis of the anticlines.

The Chancho-Co features do not fit with ground deformation contours determined from InSAR (Interferometric Synthetic Aperture Radar) studies observed by Velez et al. (2011), who describe an oval-shaped deflation feature whose location is partially coincident with Copahue volcano and also extends north-eastward over the Chancho-Co elevation. Their conceptual model is compatible with the present geochemical, geological and geophysical evidence, and deflation is regarded as a possible trigger mechanism for phreatic eruptions as those observed in the last eruptive cycles of Copahue in 1992, 1995 and 2000. The few fault-slip data measured along the reverse fault scarps indicate oblique dextral transpressional motion, consistent with the en-echélon arrangement formed by the Anfiteatro, Copahue, and Las Maquinitas depressions as well as the slightly oblique trend of the crestal grabens and open cracks with respect to the main reverse faults (Figs. 2.3 and 2.4). Melnick et al. (2006) explain the Chancho-Co kinematics due to a local rotation of the regional stress field, and they do not provide any justification for the hydrothermal activity and hot springs occurring along planes perpendicular to the greatest horizontal stress (σ_{Hmax}). In fact, Melnick et al. (2006) state that magma ascent has occurred along planes perpendicular to the least principal horizontal stress, whereas hydrothermal activity and hot springs also occur along parallel planes. The geometries of the Chancho-Co indicate that the direction of shortening was oblique to the trend of the main contractional structures (Burbank and Anderson 2001; Melnick et al. 2006). Finally, Melnick et al. (2006) suggest a tectonic control for the development of the caldera-related Chancho-Co block and of the N60 °E-trending compressive structures located on its upper part, whereas they advance the hypothesis of gravitational instability being the cause for the normal faults affecting the resurgent block.

2.3.5 The Copahue Fault

Rojas Vera et al. (2009) describe the main topographic break affecting the Chancho-Co system of reverse faults as the “Copahue

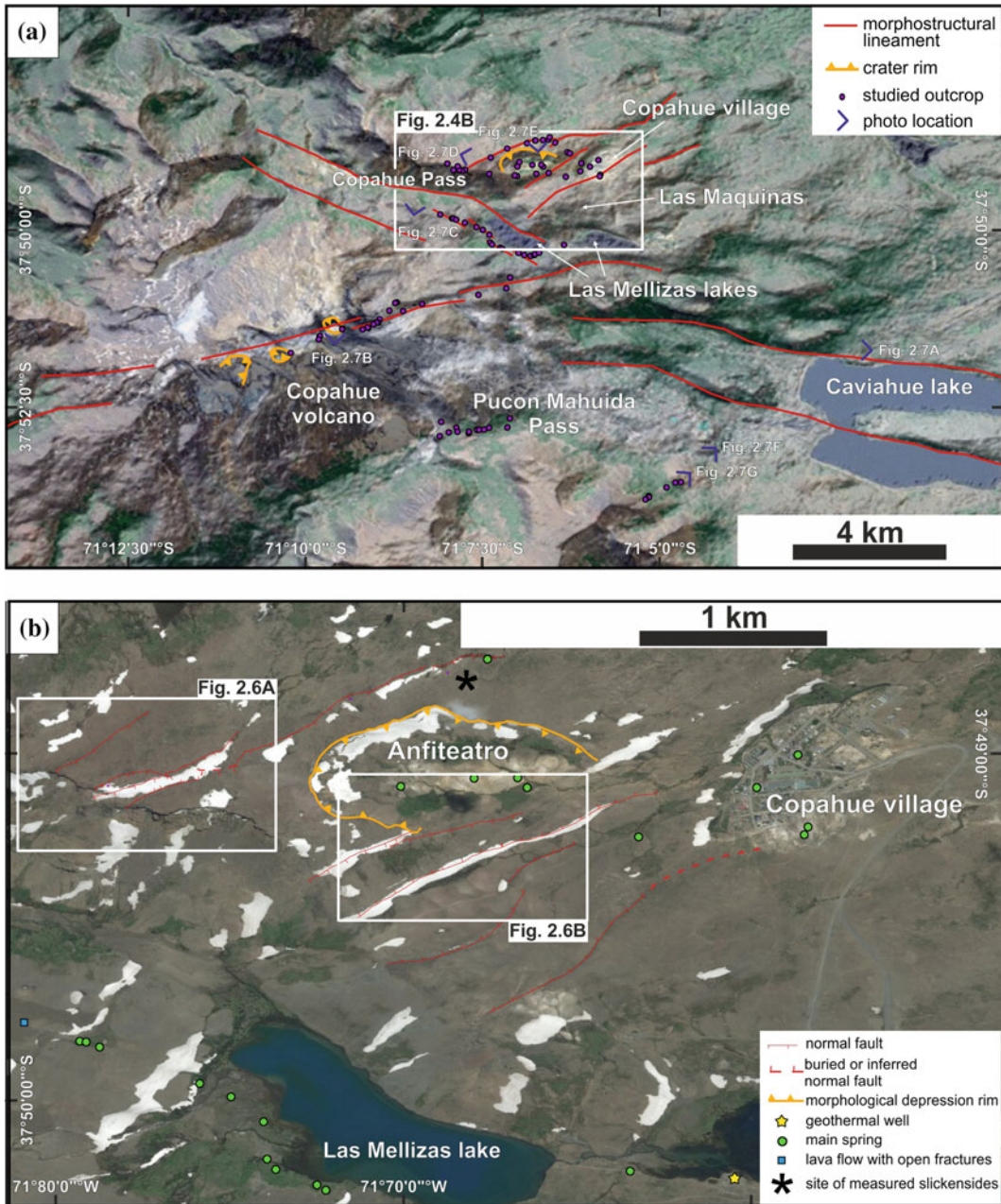


Fig. 2.4 a Morphostructural map showing the main lineaments of the area and the studied outcrops. The map contains the location of the photos illustrated in Fig. 2.7. Box locates Fig. 2.4b. b The Copahue Village

System: it affects the NE flank of Copahue volcano from Las Mellizas—Las Maquinas to Copahue Village. Boxes locate Fig. 2.6a, b

Fault”, a system of reverse (thrust) scarps to the E of Las Mellizas lakes, some of them reaching the Trolupe graben to the E (Fig. 2.3), and cutting the Copahue lavas to the SW. They also

highlight a parallelism between the uplift structures of the Chanco-Co and the alignment of post-glacial monogenetic centres and the active crater of Copahue, giving rise, as a whole, to a

fault-and-scarp system extending more than 15 km. The study of uplifted Late Pliocene sequences over younger unconsolidated fluvial and colluvial deposits enabled Rojas Vera et al. (2009) to identify at least two periods of activity for the NE-striking Copahue Fault.

2.4 Active Tectonics – New Field Data

For a better understanding of the tectonic structures that control the volcanic activity of Copahue a structural survey in December 2007 mainly devoted to the neotectonic features was carried out. The frequent eruptions of Copahue volcano, the sharp scarps along its flanks and in the surroundings, as well as the presence of abundant springs, *spa* and geothermal wells and power plants (Fig. 2.4a) suggest the presence of recent and active tectonics in the area. During the field survey, the strike of fractures, fault scarps, dikes, eruptive fissures were measured, at the same time, the abundant evidence of a structural control linked to geothermal manifestations and alteration zones were considered. By plotting direction of all measured faults, fractures, eruptive fissures and dikes (Fig. 2.5), two main tectonic trends were recognized, a dominant one oriented ENE-WSW, and a secondary ESE-WNW trend (see also Fig. 2.4a). These two trends correspond to the well known structures

affecting the CAC, as described in the previous paragraph (e.g. Folguera et al. 2004; Melnick et al. 2006; Rojas Vera et al. 2009).

The ESE-WNW-oriented structures mainly crop out along the lower northeastern flank of Copahue volcano, where the springs are aligned along this trend (Fig. 2.4b) as well as the alteration zones due to hydrothermal circulation. Along the same structure a geothermal well is in operation (Las Mellizas lake, Fig. 2.4b), and a recent lava flow shows open fractures (Fig. 2.4b). This trend results parallel to a regional one that is affecting the northern border of Copahue and shows its morphological expression also in the Caviahue lake and at the Copahue pass (Fig. 2.4a). In addition, close to the Copahue village, in the large crateric depression called Anfiteatro, two N120 °E-aligned lava domes are emplaced.

The ENE-WSW-oriented structures show a more complex trend but, at the same time, they testify to the presence of more recent activity, with open fractures, soil displacement, etc (Figs. 2.4a, b, and 2.6a, b). They were defined as the Copahue Village Fault System (CVFS—Fig. 2.4a). Such fault system partially comprises the previous defined Chanco-Co structure and Copahue Fault (Melnick et al. 2006; Rojas Vera et al. 2009), but in this case it is characterised by a different kinematics. The system is affecting Copahue volcano (Fig. 2.4a), where the summit vents and craters are aligned along a N60–70 ° E-striking trend. More specifically, in the summit

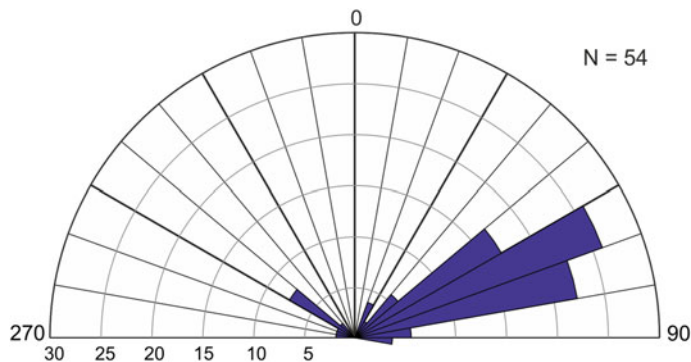


Fig. 2.5 Rose diagram showing the strike of the measured faults, fractures, eruptive fissures and dikes

area a dike strikes N60 °E (Fig. 2.7f, g). The southern rim of the summit crater lake (Fig. 2.7b) is affected by N55 °E-striking fractures, showing a left-step en-echelon arrangement. Following the same trend, on the NE flank of Copahue volcano numerous eruptive fissures are present, with a N65 °E–N78 °E-striking orientation. The Copahue village is located inside a graben with a general N60°–70 °E-striking trend and extending towards Copahue volcano (see Fig. 2.4a, b). The main graben, 3 km long and 2 km wide, is

bordered by two main normal faults, along with some minor structures that form smaller asymmetric grabens. In detail, these smaller grabens are made of several discontinuous normal faults, whose trace is usually bent, locally forming a step morphology (Fig. 2.6a, b). All the faults show normal kinematics, striking from N50 °E–N70 °E, with a vertical displacement ranging from 50 cm to 30 m, and usually of some meters, often associated with open fractures unfilled by sediments or soil. Most faults and fractures are

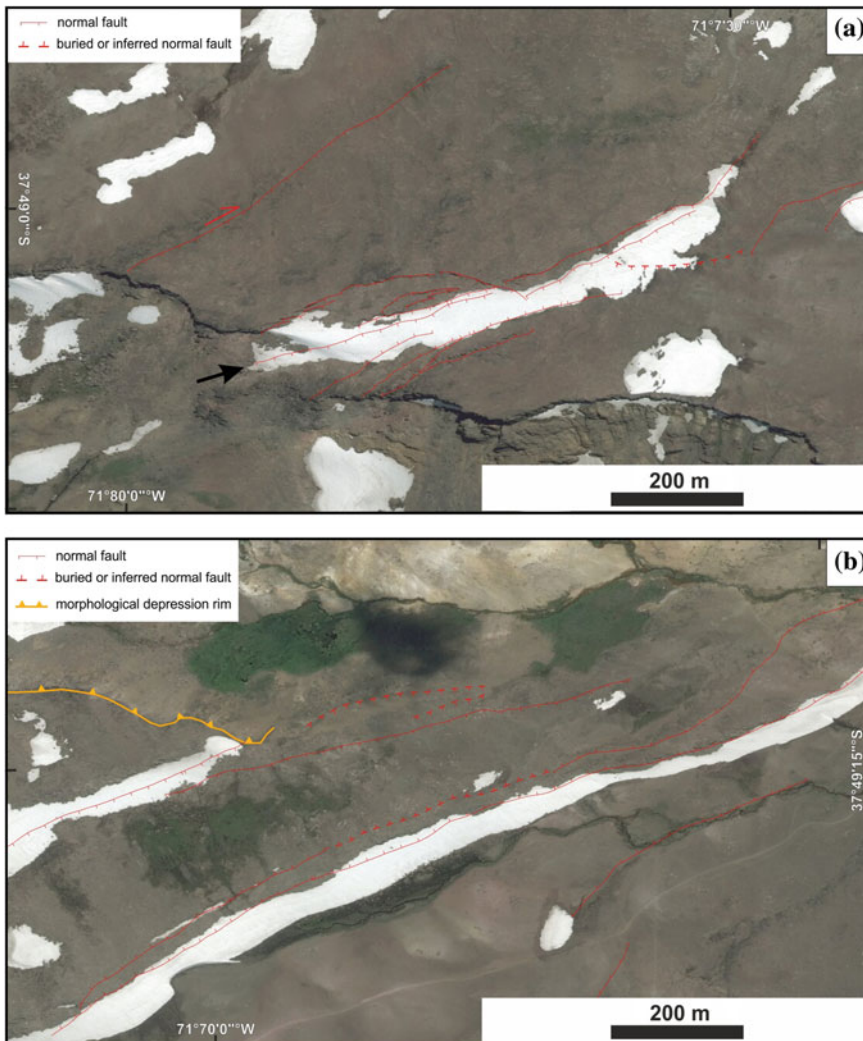


Fig. 2.6 a and b detailed sketch of the structures surveyed in two key areas. The *black arrow* in Fig. 2.6a indicates the trace of the main fault bordering the

northern side of the graben. For further explanation, please see Sect. 2.4. Location in Fig. 2.4b

also recognisable on aerial photos (Fig. 2.6a, b). Frequently, the ground is also affected by open fractures, with opening up to 20 cm, or small faults with a maximum vertical displacement of 50 cm. This is a clear evidence of ongoing tectonic deformation, as shown also by interferometric data reported in Velez et al. (2011, this book).

In addition to the normal component, the main structure bordering the northern side of the graben (see arrow in Fig. 2.6a) also shows strike-slip kinematics. In particular, close to the scarp rim, this structure presents 30 m of vertical displacement associated with a dextral strike-slip component and an estimated offset of a few centimetres, not feasible to be measured in the field (Fig. 2.7c, d). 1.5 km eastward along the structure discussed above, a sub-vertical fault plane was measured, striking N75 °E and dipping 88°, affecting a lava flow. On this fault plane slickenlines are present, and a pitch angle of 45 °W (Figs. 2.4b and 2.7e) confirms its transtensive kinematics.

In addition, two dikes belonging to the same trend were recognized, which were intruded into a fault plane along the southern wall of the Cavihue caldera, close to the Pucón Mahuida pass. They strike N47 °E–N52 °E, with a left-stepping en-échelon arrangement. One of these dikes is aphyric and 2-m-thick, the second is porphyritic and 4-m-thick, with abundant phenocrysts of plagioclase, pyroxene and olivine (Fig. 2.7f, g).

The kinematics of CVFS is transtensive, characterized by metric extensional fault scarps that border an ENE-WSW striking graben (Fig. 2.4b), associated with a minor dextral strike-slip component indicated by slickenlines, en-échelon arrangements of dikes and fractures, as shown by field and morphological observations from our work, and interferometric data (Velez et al. 2011). Therefore, the tectonic extension of the CVFS has modelled the large graben that also affects the Copahue village. This kinematics is in agreement with the estimated direction of the maximum horizontal stress in this area (N80 °E–N90 °E, Cembrano and Lara 2009). In addition, the two tectonic trends

(ENE-WSW and ESE-WNW, Figs. 2.4a and 2.5) may represent a conjugate fault system and are responsible for driving hot fluids to the surface (geothermal springs) in the area of Copahue village and Las Mellizas Lakes.

2.5 Volcano Feeding System

During the Quaternary, the volcanic activity of Copahue has concentrated along the NE-trending, 90-km-long CCM (Fig. 2.1). Such lineament is the longest of the SVZ and it is interpreted as a crustal-scale transfer zone inherited from a Miocene rifted basin (Melnick et al. 2006). In particular, along this lineament are present the N60 °E-elongated Callaqui volcano to the SW, the Copahue stratovolcano, and the Cavihue-Agrio caldera to the NE (Fig. 2.2; Moreno and Lahsen 1986; Melnick et al. 2006). Local structures formed at the intersection of regional fault systems control the volcanic activity along the CAC alignment (Melnick et al. 2006). The N60 °E-striking structural control of the CCM transfer zone is also suggested at local scale by Holocene fault scarps affecting the volcano eastern slopes as well as by post-glacial vent alignments (Fig. 2.2; Melnick et al. 2006). The Holocene activity of Copahue is testified by aligned parasitic cones, fissure-related pyroclastic flows, along with activity from the summit craters, with basaltic-andesitic products (Melnick et al. 2006). In particular, the volcano is formed by the superimposition of several emission centres along a main NE-striking fissure, and the volcano summit has nine craters aligned N60 °E, four of which post-glacial (Rojas Vera et al. 2009) and the eastern-most being presently active (Velez et al. 2011). The NE-striking fracture system affects the most recent lava flows in the NE flank of the volcano, together with the structures affecting the Chancho-Co (Rojas Vera et al. 2009). It has the same trend of the transtensive CVFS described in this chapter (cfr. 2.4). Based on the hypothesis that magmas rise along steeply-inclined intrusive sheets, propagating normal to the least principal

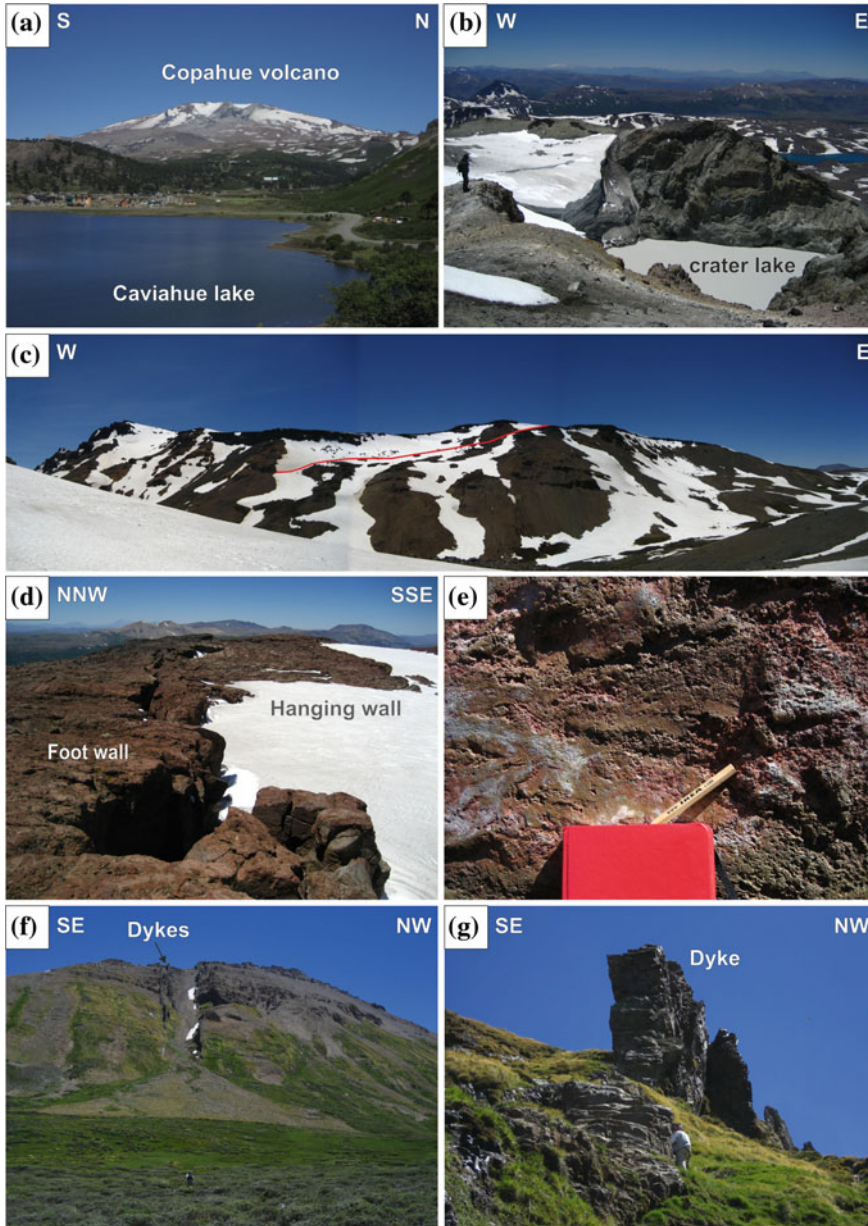


Fig. 2.7 Panoramic views and outcrops from Copahue volcano and surrounding areas. Photo location in Fig. 2.4a. **a** Copahue volcano western flank, with the village of Caviahue and the namesake lake in the foreground. **b** The summit crater of Copahue volcano, partially covered by a small ice cap. **c** Panoramic view of the Copahue Village Fault System striking ENE-WSW. The red dashed line outlines the fault plane, that corresponds to the fault indicated with black arrow in

Fig. 2.6a. **d** Close-up view of the previous fault, showing the fault displacement: footwall to the left, hanging wall, partially covered by the snow, to the right. **e** Close-up view of Copahue Village fault plane: the pencil points out the direction of the slickensides (for location, see the star in Fig. 2.4b). **f** NE-striking fault. The fault plane is intruded by dikes. **g** Close-up view of the dike striking N50 °E. For further explanation, please see Sect. 2.4

horizontal stress (σ_{Hmin}), and form dyke swarms (Dieterich 1988; Walter and Schmincke 2002) and aligned parasitic cones (Nakamura 1977; Tibaldi 1995; Corazzato and Tibaldi 2006; Bonali et al. 2011). Bonali (2013) proposed that magma at Copahue rises along vertical or sub-vertical planes striking about N60 °E, perpendicular to σ_{Hmin} (in agreement with Melnick et al. 2006). This is supported by the evidence that the Quaternary least principal stress axis (σ_3) trends NW and it is mostly sub-horizontal, as suggested by the inversion of fault-slip data between 37 °S–46 °S in the SVZ (Lavenu and Cembrano 1999; Arancibia et al. 1999; Cembrano et al. 2000; Potent and Reuther 2001; Lara et al. 2006; Cembrano and Lara 2009). Furthermore Mamani et al. (2000), based on magnetotelluric soundings, suggest the possible presence of a magma chamber at a depth between 9 and 20 km.

2.6 Elastic Interactions Between Recent Faulting and Copahue

This section explores how active tectonics is capable of influencing the normal volcanic activity at Copahue volcano. Active tectonics along the SVZ is represented by faulting that produces earthquakes both along the subduction zone and along the intra-arc active faults. Such phenomena are capable of influencing the normal volcanic activity by inducing stress changes (static, quasi static and dynamic), as suggested in the literature (Hill et al. 2002; Marzocchi et al. 2002; Manga and Brodsky 2006). Several authors pointed out that the delay between the earthquake and the following volcanic events can be from seconds to years, because of the complexity of volcanic systems (Linde and Sacks 1998; Nostro et al. 1998; McLeod and Tait 1999; Walter and Amelung 2007; Eggert and Walter 2009), despite the present lack of a thorough constraint. Regarding the SVZ, Watt et al. (2009) noticed that the overall eruption rate in the Southern Volcanic Zone (SVZ) increased after the two Chilean earthquakes of August 1906 (M_w 8.2)

and May 1960 (M_w 9.5), and this increase occurred one and 3 years after the earthquakes.

The static stress change is the variation in the stress field from just before an earthquake to shortly after the seismic waves have decayed (Hill et al. 2002). Such change is invoked as an explanation for eruption-leading processes occurring in regions close to the fault rupture (e.g., Walter and Amelung 2007; Bonali 2013; Bonali et al. 2013). Quasi-static stress change occurs over a period of years to decades, and it is associated with slow viscous relaxation of the lower crust and upper mantle beneath the epicentre of a large earthquake (Freed and Lin 2002; Marzocchi 2002a, b; Marzocchi et al. 2002). Dynamic stress, associated with the passage of seismic waves, is often regarded as a possible eruption trigger at greater distances (Linde and Sacks 1998; Manga and Brodsky 2006; Delle Donne et al. 2010).

A new method, regarding the static stress changes imparted by the earthquakes on the reconstructed volcano magma pathway (e.g. Bonali et al. 2013; Bonali 2013), was followed.

2.6.1 Conceptual Model and Modelling Strategy

In order to study a possible relationship between earthquakes and volcanic activity in the Copahue area, the normal stress change, imparted on the volcano magma pathway (e.g. Nostro et al. 1998; Walter 2007; Bonali et al. 2012) by $M_w \geq 8$ earthquakes occurred in front of the SVZ, was calculated (Bonali et al. 2013). The numerical models using the Coulomb 3.3 software (Lin and Stein 2004; Toda et al. 2005) was performed. Calculations are made in an elastic half-space with uniform isotropic elastic properties following Okada's (1992) formulae that allow to calculate the static normal stress change resolved on a volcano magma pathway, independently from the rake angle of the receiver structure and from the friction coefficient used in the model. The reconstructed magma pathway of Copahue volcano was assumed as a N60 °E-striking vertical plane, as explained in Sect. 2.5, and different

Table 2.1 Characteristics for the four $M_w \geq 8$ earthquakes and finite fault models: date of the event, magnitude, search radius, fault rupture length (Comte et al. 1986; Lomnitz 1970; Kelleher 1972; Lomnitz 1985; Okal 2005; Watt et al. 2009; Lin et al. 2013; Servicio Sismológico de la Universidad de Chile, <http://ssn.dgf.uchile.cl>; USGS earthquake hazards program), fault-plane strike and dip angle, number of patches, averaged fault slip and rake angle, depth of top and bottom of the fault plane, trend and plunge of σ_1 , σ_2 , σ_3 (based on Barrientos and Ward 1990; Lin and Stein 2004; USGS earthquake hazards program, <http://earthquake.usgs.gov>; Okal (2011), written communication; Kanamori (2011), written communication)

Name	Valparaiso	Valdivia	Santiago	Maule
Date	8/17/2006	5/22/1960	3/3/1985	2/27/2010
Mw	8.2	9.5	8.0	8.8
Rupture length (km)	330	940	170	460
Fault geometry (strike/dip, °)	8/17	7/20	11/26	8–2°/12–14
N. of patches	1	864	153	292
Average slip (m)	2.6	3.8	1.6	2.5
Average rake angle (°)	117.0	105.0	105.0	105.0
Fault top (km)	20.5	0.0	21.8	2.9
Fault bottom (km)	47.5	153.9	61.3	50.1
σ_1 (azimuth/plunge, °)	71/31	100/35	86/20	92/28
σ_2 (azimuth/plunge, °)	157/7	10/0	174/9	178/5
σ_3 (azimuth/plunge, °)	56/58	80/55	61/68	80/61

attitudes were also tested by changing the dip angles (50°, 70° and 90°). Its reconstructed geometry also mimics the Quaternary geometry of active faults reported in this work, striking ENE-WSW. The upper crust was modelled as an elastic isotropic half-space characterized by a Young's modulus $E = 80$ GPa and a Poisson's ratio $\nu = 0.25$ based on Mithen (1982), King et al. (1994), Lin and Stein (2004) and Toda et al. (2005); a lower value of the Young's modulus would only have the effect of reducing the magnitude of static stress changes. Regarding the finite fault model used to simulate earthquake effects, for the 1960 earthquake the fault solutions proposed by Barrientos and Ward (1990) based on tsunami wave form inversion was used, whereas for the 2010 earthquake the fault solutions proposed by Lin et al. (2013), based on InSAR, GPS and teleseismic data, was used. The input stress field for both earthquakes is reported in Table 2.1, based on T, N and P axis of related focal mechanisms. Furthermore, it has been evaluated the possible contribution of earthquake-induced static stress changes due to crustal earthquakes occurred between the 1907

and the 2010 Chile earthquakes available in a digital database provided by USGS (<http://earthquake.usgs.gov>). Fault geometries and kinematics are based on focal mechanism solutions (<http://earthquake.usgs.gov>; <http://www.gmtproject.it/>) when available, and geometries and kinematics of active faults reported in the literature (Melnick et al. 2006; Cembrano and Lara 2009). Fault dimensions were based on empirical relations (Wells and Coppersmith 1994; Toda et al. 2011). The earthquake-induced normal stress changes on Copahue feeding system, possibly imparted by earthquakes with $M_w \geq 4$ and a depth between 0 and 70 km (<http://earthquake.usgs.gov>), was also resolved.

2.6.2 Interaction Between the Subduction Zone and the Volcano

It is commonly suggested that large subduction earthquakes are capable of inducing static stress perturbations on the fault hanging wall block, also promoting volcanic eruptions (Barrientos 1994; Lin and Stein 2004; Walter and Amelung

2007; Bonali 2013; Bonali et al. 2013). Static stress change is the difference in the stress field from just before an earthquake to shortly after the seismic waves have decayed (Hill et al. 2002), and it is proposed as a mechanism capable of leading eruptions in regions close to the fault rupture (e.g., Walter and Amelung 2007; Bonali et al. 2013). Although a first theory suggested that magma could be squeezed upward by increased compressional stress in the crust surrounding a magma chamber close to its critical state (e.g. Bautista et al. 1996), more recent findings agreed that earthquake-induced static (permanent) normal stress reduction on magma pathway (unclamping) could promote dyke intrusion and following eruptions (e.g. Hill et al. 2002; Walter 2007). Furthermore, Walter and Amelung (2007) suggested that earthquake-induced volumetric expansion can increase the magma-gas pressure and encourage eruptions in a time frame of years. Finally, Bonali et al. (2013) advanced the hypothesis that unrest at volcanoes with deep magma chambers is encouraged by magma pathway unclamping.

Results of numerical modelling suggest that both the 1960 and 2010 subduction earthquakes were capable of inducing unclamping at vertical or subvertical magma pathway of Copahue volcano (Fig. 2.8). Regarding the 1960 earthquake-induced static stress changes (Fig. 2.8a, b), unclamping is higher for a vertical or SE-dipping magma pathway and it increases with depth, while it decreases with depth for a NW-dipping magma pathway, and it results in clamping at a depth between 5–9 km for the 50°-NW-dipping pathway (Fig. 2.8b). Regarding the 2010 earthquake-induced static stress changes, the magma pathway (Fig. 2.8c) is always affected by a normal stress reduction (unclamping) within a depth range of 1–9 km below the volcano base (Fig. 2.8d). Magnitude of unclamping slightly decreases with depth, and ranges from -0.258 to -0.147 MPa (Bonali 2013), and decreases with decreasing dip angle of the magma pathway (Fig. 2.8d). Although positive feedbacks due to dynamic and post-seismic stress changes could not be excluded, large subduction earthquakes seems to be capable of favouring volcanic

activity at Copahue due to earthquake-induced static (permanent) normal stress reduction on its magma pathway (e.g. Hill et al. 2002; Walter 2007) at a distance of 257–353 km and up to 3 years following subduction earthquakes (Bonali 2013; Bonali et al. 2013). Such hypothesis is supported by some suggestion proposed in Marzocchi (2002a, b) where coseismic stress changes are candidate to promote eruptions in the 0–5 years after earthquakes as far as 100–300 km from the epicentre (i.e. 38 h after the 1960 Valdivia 9.5 M_w earthquake the Cordon Caulle erupted; Moreno and Petit-Breuilh 1999, Collini et al. 2013). Regarding the time delay, Marzocchi (2002a, b) has proposed that: (i) the inertia of the volcanic system in reacting to the static stress changes, (ii) a non perfect elasticity of the crust and/or (iii) stress corrosion effect (e.g., Main and Meredith 1991), are processes candidate to explain a time delay of 0–5 years. Other mechanisms that could have promoted unrest at Copahue, following such earthquakes, regard postseismic-induced stress/strain (Marzocchi 2002a, b; Marzocchi et al. 2002) and dynamic stress changes (Manga and Brodsky 2006). As proposed by Marzocchi et al. (2002) and Freed and Lin (2002), quasi-static stress change, which is a post-seismically-induced effect, could promote eruptions over a period of years to decades. Marzocchi (2002a, b) suggested a time window of about 30–35 years after earthquakes, compatibly to the relaxation time of a viscous asthenosphere (Piersanti et al. 1995, 1997; Pollitz et al. 1998; Kenner and Segall 2000). Regarding the dynamic stress changes, such effects may excite and promote ascent of gas bubbles, and consequently magma ascent (Manga and Brodsky 2006), the details of the feedback mechanisms remaining unclear and are nowadays discussed in the literature. It is proposed that dynamic effects is capable of promoting bubble growth, including adjective overpressure (Linde et al. 1994), rectified diffusion (Brodsky et al. 1998; Ichihara and Brodsky 2006) and shear strain (Sumita and Manga 2008). Copahue experienced 9 eruptions since 1900 (Global Volcanism Program Digital Information Series), five of which in the last 21 years (Fig. 2.9). In

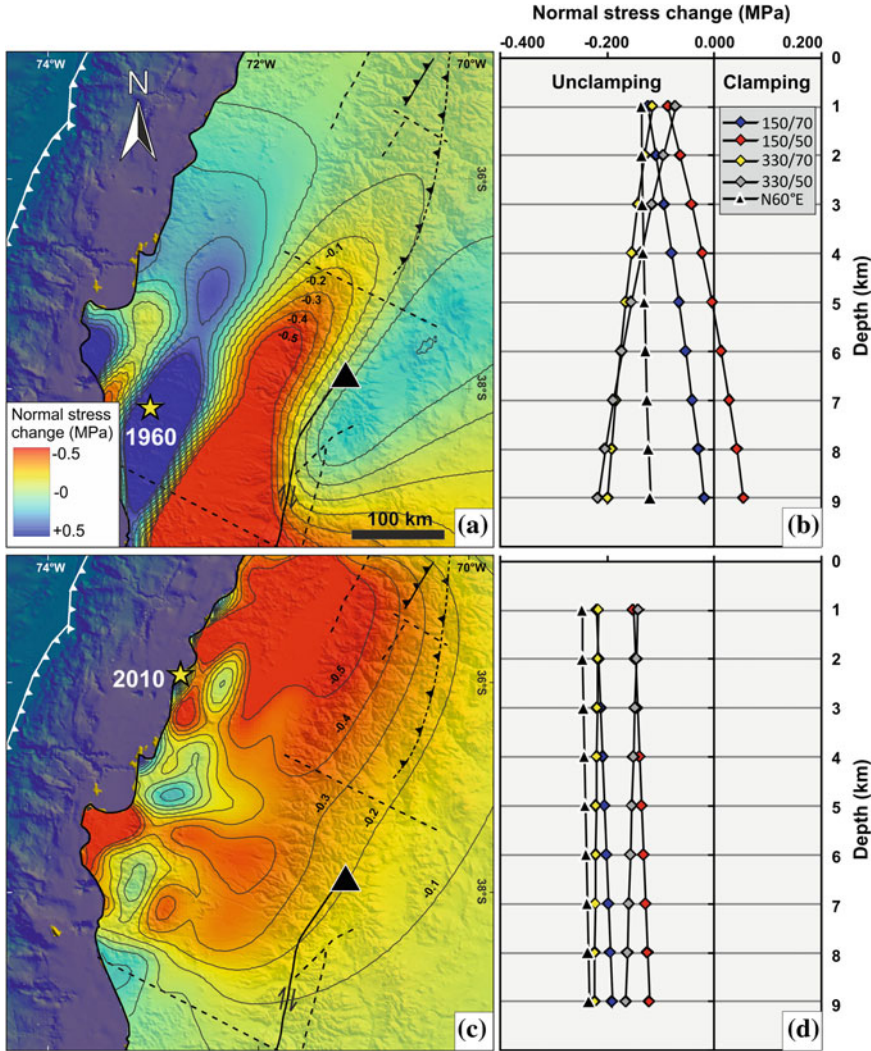


Fig. 2.8 **a** Contour map of the 1960 M_w 9.5 earthquake-induced normal stress change resolved on the N60 °E-striking Copahue magma pathway at a depth of 4.5 km below the volcano base. Red colours represent a normal static stress reduction on the receiver plane, blue colours represent an increase. The black triangle locates Copahue volcano. The finite fault model used is from Barrientos and Ward (1990), and **b** shows the normal stress change for vertical as well as inclined receiver

surfaces (attitude expressed as dip direction/dip angle), in a depth range of 1–9 km below the volcano. **c** Contour map of the M_w 8.8 2010 earthquake-induced normal stress change resolved on the N60 °E-striking Copahue magma pathway at a depth of 4.5 km below the volcano base. The finite fault model used here is from Lin et al. (2013), and **d** shows the normal stress change for vertical as well as inclined receiver surfaces in a depth range of 1–9 km below the volcano

detail, four eruptions occurred in the time-frame 1992–2000, the recentmost eruption (2012) occurred instead after the 2010 Chile earthquake, under unclamping conditions of the magma

pathway. The Copahue magma pathway was affected by normal stress reduction also after the 1960 Valdivia earthquake, and the volcano erupted certainly in 1961.

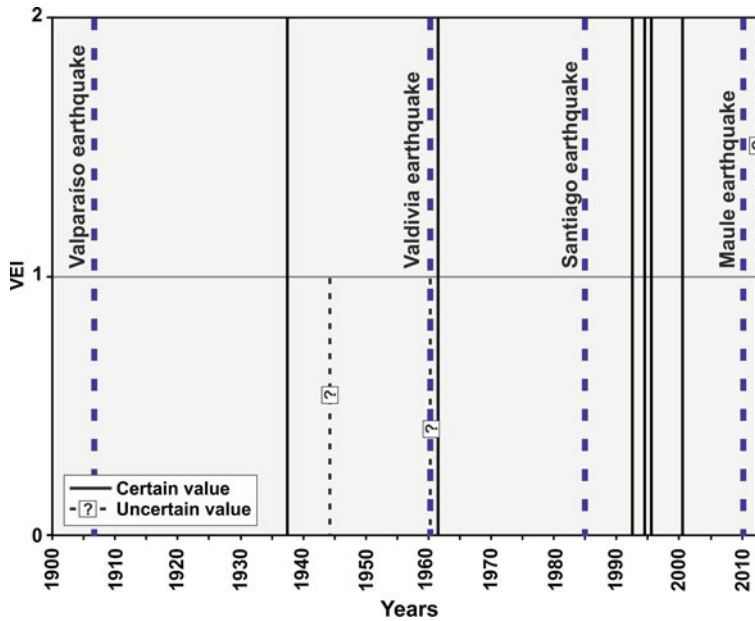


Fig. 2.9 The graph reports the eruptions occurred at Copahue since 1900 AD (Global Volcanism Program Digital Information Series) and significant earthquakes

($M_w > 8$) along the SVZ. Marks represent the first day of each reported year. VEI-Volcanic Explosivity Index

2.6.3 Effect of the Surrounding Structures on the Volcano

Our analysis of the possible contribution of earthquake-induced static stress changes due to crustal earthquakes with M_w 4–6.6 (<http://earthquake.usgs.gov>) reveals that only one out of 2727 earthquakes (Fig. 2.10a) was capable of inducing static normal stress changes on the Copahue magma pathway (Fig. 2.10b). Such earthquake occurred on 31/12/2006 with M_w of 5.6 at a distance of about 11 km from the volcano. The hypocenter was 20.6 km deep (<http://earthquake.usgs.gov>) and the kinematics was dextral strike-slip (Fig. 2.10a). Results of the numerical modelling carried out considering different dip angles of the N60 °E-striking magma pathway suggest that such surface suffered a normal stress reduction when vertical or subvertical, SE-dipping. A subvertical NW-dipping pathway is instead sometimes affected by normal stress increase with depth. When considering a less inclined NW-dipping pathway, no relevant normal stress changes are observed (Fig. 2.10b). Whatever the case, the

stress change imparted by the 2010 earthquake is two orders of magnitude greater than the contribution of the 2006 seismic event.

2.7 Discussion

The role of structures in a volcanic area is unquestionable because they control the magma storage and drive the magma rising, as well as the location of vents and the evolution of a volcano (e.g. Bellotti et al. 2006; Norini et al. 2013). In this way, by examining the structural data published up to now on Copahue volcano (see Sect. 2.3), it is evident that a comprehensive model is lacking and a large discussion is ongoing. In this section, all these available data were summarised, showing that there are some divergences among them and the related models. In addition, the new field data presented here (see Sect. 2.4), which cover only some portions of the volcanic area and consider mainly the recent and present volcano-tectonic activity, were considered.

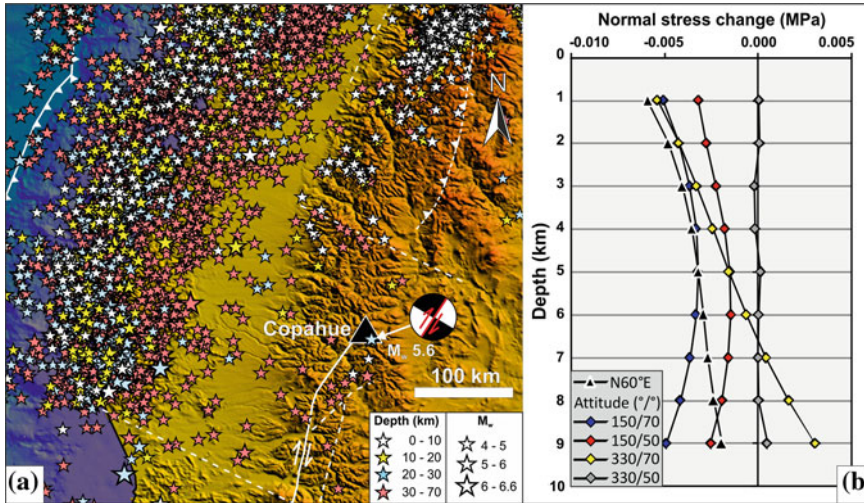


Fig. 2.10 **a** Stars represent the crustal earthquakes with $M_w \geq 4$ (<http://earthquake.usgs.gov>) occurred in the time-frame between the 1907 and the 2010 Chile earthquake. The focal mechanism of 31/12/2006 (M_w 5.6) is shown (<http://earthquake.usgs.gov>; <http://www.gmtproject.it/>), the red line representing fault strike and kinematics (Melnick et al. 2006; Cembrano and Lara

2009). **b** 2006 M_w 5.6 earthquake-induced normal stress change resolved on the N60 °E-striking reconstructed Copahue magma pathway. Vertical as well as inclined receiver surfaces are taken into account (attitude expressed as dip direction/dip angle), in a depth range of 1–9 km below the volcano

The long geological history of this sector of the Andes results in a really complex pattern of structures, with the superimposition of different tectonic phases. In detail, the complex structural setting displayed by Melnick et al. (2006) (Fig. 2.3) shows the presence of several generations of faults because of the variable position in time and somewhere in space of σ_{hmax} in the entire area. South of Copahue volcano there is a set of structures parallel to each others, striking NNE-SSW and with conflicting kinematics, as strike-slip faults parallel to normal faults and folds (anticlines and synclines). In addition, perpendicular to this direction a thrust system is emplaced. These features cannot be easily reconciled and could be explained to be the result of two or more generations of structures and/or of the heritage of older phases. Also in the Anfiteatro area, close to the Copahue village, there is another evident incompatibility between a set of reverse faults associated with fold anticlines and the normal faults parallel to them, and the geothermal field alignment (Melnick et al. 2006, Fig. 2.3).

In view of the main structures affecting Copahue volcano there is a general agreement among the authors that the ENE-WSW-striking lineament is the most important, because of active vents and summit craters alignment. This feature represents the local expression of the regional CMC structure (Figs. 2.1, 2.2, 2.3 and 2.4), a transfer fault system that links the LOFZ to the ACFZ (Folguera and Ramos 2009; Velez et al. 2011) along with three volcanoes are located (Callaqui, Copahue and Mandolegue). This fault system extends in the area close to the Copahue Village and Anfiteatro where vertical displacements, mainly reversal, associated with a right-lateral component have been identified. Some of these structures are named Chanco-Co and Copahue Fault (Fig. 2.3) (e.g. Folguera et al. 2004; Melnick et al. 2006; Rojas Vera et al. 2009 with some differences among their models). In our neotectonic survey (Figs. 2.4, 2.6 and 2.7) any evidence of recent reverse faults was identified; instead, based on our field data, they were considered as normal faults with a dextral strike-slip component. The subvertical geometry

of the faults (and their graben-like arrangement), the displacements, the presence of open fractures (up to 20 cm wide) and the few slickenlines suggest a normal-oblique kinematics for these structures. This normal fault system was named as Copahue Village Fault System (CVFS) was finally proposed. The CVFS kinematics is in agreement with the deflation observed by Velez et al. (2011), confirming that these are the recentmost structures in the area, and thus they are more recent than the Chanco-Co structure. As suggested by Melnick et al. (2006), no evidence of folds on the topographic surface was identified; the lava flows display a tabular geometry, and local folding can be explained with the rotation due to the normal movements (drag) along the fault plane. The coeval presence of fold anticlines and parallel reverse faults can be related to the same stress field, but in this case the σ_{hmax} has to be rotated (about 90°) with respect to the regional one (N80 °E–N90 °E; Cembrano and Lara 2009). On the contrary, considering the new structural data, the resulting σ_{hmax} is in agreement with the regional one and the main geothermal sources are located in extensional and transtensional settings associated to a general deflation observed by InSAR data (Velez et al. 2011). Another evidence of extensional regime for the CVFS is suggested by the geometry of the plumbing system, striking almost parallel to this fault system. A previous shortening phase marked by folds and thrusts cannot be excluded, as recognised in the field and described in many outcrops by, among the others, Folguera et al. (2004), Melnick et al. (2006) and Rojas Vera et al. (2009). Conversely, the normal pattern recognised in our recent survey close to the Anfiteatro needs to be confirmed by more extensive surveys, also to recognise possible diverse recent tectonic phases. Taking into account all the available data and models proposed for the area close to the Copahue village, an in-depth study appears necessary to better understand the structural setting and its evolution, allowing to recognise two or more possible tectonic phases. In addition, further studies should address the determination of the displacement rate of the active structures, because of

their importance for volcanic and seismic hazard and for geothermal exploitation.

Results of numerical models show that active tectonics is capable of perturbing the normal activity at Copahue due to static stress transfer. In the studied cases both 1960 and 2010 subduction earthquakes induced a normal stress reduction on volcano magma pathway, favouring dyke intrusion (e.g., Hill et al. 2002; Walter 2007; Walter and Amelung 2007). Minor events, occurred along intra-arc faults, were also capable of producing the same effect, but with minor intensity.

2.8 Final Remarks

This review presents the state-of-art about tectonic data in the CAC and surroundings area as well as includes some new neotectonic data around Copahue volcano. The main points are summarised as follow:

1. Different structural models have been proposed right now, but a comprehensive model is lacking and further in-depth studies are necessary.
2. A main ENE-WSW striking structure affects Copahue volcano and represents the local expression of the CCM transfer zone. This structure is inferred to control the magma pathway and the volcano evolution. There is no agreement on the normal or reverse kinematics related to the present activity of the CVFS. The possible reverse movement of this fault system needs a rotation of the regional σ_{hmax} , while the normal one is in agreement with it.
3. A better knowledge of the CVFS activity, the potential presence of two or more phases and the understanding of its Holocenic strain rate are fundamental goals for further and in-depth structural studies. In fact, a more detailed and complete tectonic setting of the CAC should represent a fundamental result also for the general geological-structural model of this area, providing structural constraints for the

magma storage, pathway and rising, and representing an essential issue also for volcanic hazard assessment, as well as for enhancing the exploitation of the geothermal system.

4. Active tectonics is capable of perturbing the normal activity at Copahue volcano due to earthquake-induced static stress changes. As result of numerical modelling, both 1960 and 2010 large subduction earthquakes induced unclamping on Copahue feeding system, favouring following eruptions. Very low unclamping was also induced by one crustal earthquake occurred after the pre-2012 eruption and before the 2010 earthquake.

Acknowledgments Fieldwork in the Copahue area was carried out in the framework and with funding of the IGCP 508YS Project “Inception of volcano collapses by fault activity: examples from Argentina, Ecuador and Italy” co-led by C. Corazzato, and benefited also from a TWAS grant. The authors thank Ivan Petrinovic for field cooperation. We acknowledge Ross E. Stein, Jian Lin and Min Ding for providing the Coulomb input file for the 1960 Chile earthquake. Hiroo Kanamori kindly provided the focal mechanism data for the 1960. Anthony Sladen is acknowledged for kindly providing the 2010 Chile earthquake finite fault models. We also want to thank the Editors for inviting us in the thematic volume and for their kind support, and Marco Bonini and José Viramonte, whose comments improved the paper.

References

- Adriasola AC, Thomson SN, Brix MR, Hervé F, Stockhert B (2006) Postmagmatic cooling and Late Cenozoic denudation of the North Patagonian Batholith in the Los Lagos Region of Chile, 41°S–42°S. *Int J Earth Sci* 95:504–528
- Arancibia G, Cembrano J, Lavenu A (1999) Transpresión dextral y partición de la deformación en la Zona de Falla Liquiñe-Ofqui, Aisén, Chile (44–45°S). *Rev Geol Chile* 26(1):3–22
- Barrientos SE, Ward SN (1990) The 1960 Chile earthquake; inversion for slip distribution from surface deformation. *Geophys J Intern* 103:589–598
- Barrientos SE (1994) Large thrust earthquakes and volcanic eruptions. *Pure appl Geophys* 142(1):225–237
- Bautista BC, Bautista MLP, Stein RS, Barcelona ES, Punongbayan RS, Laguerta AR, Rasdas EP, Ambubuyog G, Amin EQ (1996) Relationship of regional and local structures of Mount Pinatubo activity. In: Newhall CG, Punongbayan RS (eds) *Fire and mud: Eruptions and Lahars of Mount Pinatubo, Philippines*. University of Washington Press, Seattle, pp 351–370
- Bebbington MS, Marzocchi W (2011) Stochastic models for earthquake triggering of volcanic eruptions. *J Geophys Res* 116:B05204. doi.org/10.1029/2010JB008114
- Bellotti F, Capra L, Groppelli G, Norini G (2006) Tectonic evolution of the central-eastern sector of trans Mexican volcanic belt and its influence on the eruptive history of the Nevado de Toluca Volcano (Mexico). In: Tibaldi A, Lagmay AMF (eds) *Interaction between volcanoes and their basement*. *J Volcanol Geotherm Res* 158:21–36
- Bonali FL, Corazzato C, Tibaldi A (2011) Identifying rift zones on volcanoes: an example from La Réunion island. *Indian Ocean Bull Volcanol* 73(3):347–366
- Bonali FL, Corazzato C, Tibaldi A (2012) Elastic stress interaction between faulting and volcanism in the Olacapato-San Antonio de Los Cobres area (Puna plateau, Argentina). *Global Planet Change* 90–91:104–120
- Bonali FL (2013) Earthquake-induced static stress change on magma pathway in promoting the 2012 Copahue eruption. *Tectonophysics* 608:127–137
- Bonali FL, Tibaldi A, Corazzato C, Tormey DR, Lara LE (2013) Quantifying the effect of large earthquakes in promoting eruptions due to stress changes on magma pathway: the Chile case. *Tectonophysics* 583:54–67
- Brodsky EE, Sturtevant B, Kanamori H (1998) Earthquakes, volcanoes, and rectified diffusion. *Geophys Res Lett* 103:23827–23838
- Broggi A, Liotta D, Meccheri M, Fabbrini L (2010) Transensional shear zones controlling volcanic eruptions: the Middle Pleistocene Mt Amiata volcano (inner Northern Apennines, Italy). *Terra Nova* 22(2):137–146
- Burbank DW, Anderson RS (2001) *Tectonic geomorphology*. Blackwell Scientific, Oxford, p 270
- Cameli GM, Dini I, Liotta D (1993) Upper crustal structure of the Larderello geothermal field as a feature of post-collisional extensional tectonics (southern Tuscany, Italy). *Tectonophysics* 224(4):413–423
- Cembrano J, Hervé F, Lavenu A, Shermer E, Lavenu A, Sanhueza A (1996) The Liquiñe Ofqui fault zone: a long-lived intra-arc fault system in southern Chile. *Tectonophysics* 259(1–3):55–66
- Cembrano J, Shermer E, Lavenu A, Sanhueza A (2000) Contrasting nature of deformation along an intra-arc shear zone, the Liquiñe-Ofqui fault zone, southern Chilean Andes. *Tectonophysics* 319:129–149
- Cembrano J, Lara L (2009) The link between volcanism and tectonics in the Southern Volcanic Zone of the Chilean Andes: a review. *Tectonophysics* 471:96–113
- Chinn DS, Isacks BL (1983) Accurate source depths and focal mechanisms of shallow earthquakes in western South America and in the News Hebrides islands arc. *Tectonics* 2:529–563
- Cisternas M, Atwater BF, Torrejon T, Sawai Y, Machuca G, Lagos M, Eipert A, Youlton C, Ignacio S, Kamataki T, Shishikura M, Rajendran CP, Malik JK,

- Rizal Y, Husni M (2005) Predecessors of the giant 1960 Chile earthquake. *Nature* 437:404–407
- Collini E, Osores MS, Folch A, Viramonte JG, Villarosa G, Salmuni G (2013) Volcanic ash forecast during the June 2011 Cordon Caulle eruption. *Nat Haz* 66(2):389–412. doi:10.0007/s11069-012-0492-y
- Comte D, Eisenberg A, Lorca E, Pardo M, Ponce L, Saragoni R, Singh SK, Suárez G (1986) The central Chile earthquake of 3 March 1985: a repeat of previous great earthquakes in the region? *Science* 233:449–453
- Corazzato C, Tibaldi A (2006) Basement fracture control on type, distribution, and morphology of parasitic volcanic cones: an example from Mt. Etna, Italy. In: Tibaldi A, Lagmay M (eds) Interaction between Volcanoes and their Basement. *J Volcanol Geoth Res Special issue*, 158:177–194
- Decker RW, Klein FW, Okamura AT, Okubo PG (1995) Forecasting eruptions of Mauna Loa Volcano, Hawaii. Mauna Loa revealed; structure, composition, history, and hazards. American Geophysical Union, Washington, DC, United States, pp 337–348
- Delle Donne D, Harris AJL, Ripepe M, Wright R (2010) Earthquake-induced thermal anomalies at active volcanoes. *Geology* 38(9):771–774
- Dieterich JH (1988) Growth and persistence of Hawaiian volcanic rift zones. *J Geophys Res* 93:4258–4270
- Eggert S, Walter TR (2009) Volcanic activity before and after large tectonic earthquakes: observations and statistical significance. *Tectonophysics* 471:14–26
- Folguera A, Ramos VA (2000) Control estructural del volcán Copaua: Implicancias tectónicas para el arco volcánico Cuaternario (36°–39 °S). *Rev Geol Arg* 55:229–244
- Folguera A, Ramos VA (2009) Collision of the Mocha fracture zone and a < 4 Ma old wave of orogenic uplift in the Andes (36°–38 °S). *Lithosphere* 1(6):364–369
- Folguera A, Ramos VA, Zelnick D (2002) Partición de la deformación en la zona del arco volcánico de los Andes neuquinos (36–39 °S) en los últimos 30 millones de años. *Rev Geol Chile* 29(2):151–165
- Folguera A, Ramos VA, Hermans R, Naranjo J (2004) Neotectonics in the foothills of the southernmost central Andes (37°–38 °S): Evidence of strike-slip displacement along the Antñir-Copahue fault Zone. *Tectonics* 23(5). doi:10.1029/2003TC001533
- Folguera A, Ramos VA, Gonzalez Diaz E, Hermanns R (2006) Late Cenozoic evolution of the Eastern Andean Foothills of Neuquén between 37° and 37°30'S. In: Kay SM, Ramos VA (eds) Late Cretaceous to recent magmatism and tectonism of the Southern Andean Margin at the latitude of the Neuquén Basin (36–39 ° S). *Geol Soc Am* 407:247–266
- Folguera A, Rojas Vera E, Tobal J, Orts D, Ramos VA (2015) A review to the geology, structural controls and tectonic setting of the Copahue volcano in the Southern Volcanic Zone (in this volume 2015)
- Freed AM, Lin J (2002) Accelerated stress buildup on the southern San Andreas Fault and surrounding regions caused by Mojave Desert earthquakes. *Geology* 30(6):571–574
- Giordano G, Pinton A, Cianfarra P, Baez W, Chiodi A, Viramonte J, Norini G, Gropelli G (2013) Structural control on geothermal circulation in the Cerro Tuzgle-Tocomar geothermal volcanic area (Puna plateau, Argentina). *J Volcanol Geotherm Res* 249:77–94
- Gropelli G, Norini G (2011) Geology and tectonics of the southwestern boundary of the unstable sector of Mt Etna (Italy). *J Volcanol Geotherm Res* 208:66–75
- Hill DP, Pollitz F, Newhall C (2002) Earthquake-volcano interactions. *Phys Today* 55:41–47
- Ibáñez JM, Del Pezzo E, Bengoa C, Caselli A, Badi G, Almendros J (2008) Volcanic tremor and local earthquakes at Copahue volcanic complex, Southern Andes, Argentina. *J Volcanol Geotherm Res* 174:284–294
- Ichihara M, Brodsky EE (2006) A limit on the effect of rectified diffusion in volcanic systems. *Geophys Res Lett* 33:L02316. doi.org/10.1029/2005GL024753
- Invernizzi C, Pierantoni PP, Chiodi A, Maffucci R, Corrado S, Baez W, Tassi F, Giordano G, Viramonte J (2014) Preliminary assessment of the geothermal potential of Rosario de la Frontera area (Salta, NW Argentina): insight from hydro-geological, hydro-geochemical and structural investigations. *J South Am Earth Sci* 54:20–36
- Kelleher JA (1972) Rupture zones of large South American earthquakes and some predictions. *J Geophys Res* 77:2087–2103
- Kenner SJ, Segall P (2000) Postseismic deformation following the 1906 San Francisco earthquake. *J Geophys Res* 105:13195–13209
- King GCP, Stein RS, Lin J (1994) Static stress changes and the triggering of earthquakes. *Bull Seismol Soc Am* 84:935–953
- Lange D, Cembrano J, Rietbrock A, Haberland C, Dahm T, Bataille K (2008) First seismic record for intra-arc strike-slip tectonics along the Liquiñe-Ofqui fault zone at the obliquely convergent plate margin of the southern Andes. *Tectonophysics* 455:14–24
- Lara LE, Lavenu A, Cembrano J, Rodríguez C (2006) Structural controls of volcanism in transversal chains: resheared faults and neotectonics in the Cordón Caulle-Puyehue area (40.5 °S), southern Andes. *J Volcanol Geotherm Res* 158:70–86
- Lavenu A, Cembrano J (1999) Compressional and transpressional-stress pattern for Pliocene and Quaternary brittle deformation in fore and intra-arc zones (Andes of Central and Southern Chile). *J Structur Geol* 21:1669–1691
- Lin J, Stein RS (2004) Stress triggering in thrust and subduction earthquakes, and stress interaction between the southern San Andreas and nearby thrust and strike-slip faults. *J Geophys Res* 109:B02303
- Lin YN, Sladen A, Ortega-Culaciati F, Simons M, Avouac J-P, Fielding EJ, Brooks BA, Bevis M, Genrich J, Rietbrock A, Vigny C, Smalley R, Socquet A (2013) Coseismic and postseismic slip

- associated with the 2010 Maule earthquake, Chile: characterizing the Arauco Peninsula barrier effect. *J Geophys Res* 118(6):3142–3159
- Linde AT, Sacks IS (1998) Triggering of volcanic eruptions. *Nature* 395:888–890
- Linde AT, Sacks IS, Johnston MJS, Hill DP, Bilham RG (1994) Increased pressure from rising bubbles as a mechanism for remotely triggered seismicity. *Nature* 371:408–410
- Lomnitz C (1970) Major earthquakes and tsunamis in Chile during the period 1535 to 1955. *Geologische Rundschau Zeitschrift für Allgemeine Geologische* 59:938–960
- Lomnitz C (1985) Tectonic feedback and the earthquake cycle. *Pageoph* 123:667–682
- López-Escobar L, Cembrano J, Moreno H (1995) Geochemistry and tectonics of the Chilean Southern Andes basaltic quaternary volcanism (37–46 °S). *Rev Geol Chile* 22(2):219–234
- Main IG, Meredith PG (1991) Stress corrosion constitutive laws as a possible mechanism of intermediate-term and short-term seismic quiescence. *Geophys J Int* 107:363–372
- Mamani MJ, Borzotta E, Venencia JE, Maidana A, Moyano CE, Castiglione B (2000) Electric structure of the Copahue Volcano (Neuquén Province, Argentina), from magnetotelluric soundings: 1D and 2D modelings. *J South Am Earth Sci* 13:147–156
- Manga M, Brodsky EE (2006) Seismic triggering of eruptions in the far field: volcanoes and geysers. *Annual Review of Earth and Planetary Science*, 34, 263–291
- Marzocchi W (2002a) Remote seismic influence on large explosive eruptions. *J Geophys Res* 107(B1): 2018
- Marzocchi W (2002b) Remote seismic influence on the large explosive eruptions. *J Geophys Res* 107:EPM 6–1
- Marzocchi W, Scandone R, Mulargia F (1993) The tectonic setting of Mount Vesuvius and the correlation between its eruptions and the earthquakes of the Southern Apennines. *J Volcanol Geotherm Res* 58(1–4):27–41
- Marzocchi W, Casarotti E, Piersanti A (2002) Modeling the stress variations induced by great earthquakes on the largest volcanic eruptions of the 20th century. *J Geophys Res* 107(B11):2320
- Mazzoni MM, Licitra DT (2000) Significado estratigráfico y volcanológico de depósitos de flujos piroclásticos neógenos con composición intermedia en la zona del lago Caviahue, provincia del Neuquén. *Rev Asoc Geol Arg* 55(3):188–200
- McLeod P, Tait S (1999) The growth of dykes from magma chambers. *J Volcanol Geotherm Res* 92:231–246
- Melnick D (2000) Geometría y estructuras de la parte norte de la zona de falla de Liquiñe-Ofqui (38°S): interpretación de sensores remotos. In: IX Congreso Geológico Chileno, Puerto Varas, Chile, vol 1, pp 796–799
- Melnick D, Folguera A (2001) Geología del complejo volcánico Copahue-Caldera Del Agrío, un sistema transtensional activo desde el Plioceno en la transición de los Andes Patagónicos a los Andes Centrales (38 ° S–71 °O). In: IX Congreso Geológico Latinoamericano, Montevideo, Uruguay, Universidad de Montevideo, pp 6–11
- Melnick D, Folguera A, Ramos VA (2006) Structural control on arc volcanism: the Caviahue-Copahue complex, Central to Patagonian Andes transition (38 °S). *J South Am Earth Sci* 22:66–88
- Moreno H, Lahsen A (1986) El volcán Callaqui: ejemplo de vulcanismo fisural en los Andes del Sur. *Rev Asoc Geol Arg* 42:1–8
- Moreno H, Petit-Breuilh ME (1999) El volcán fisural CórdónCaulle, Andes del Sur (40.5°S): geología general y comportamiento eruptivo histórico. In: XIV Congreso Geológico Argentino, Córdoba, Argentina, vol 2, pp 258–260
- Mithen DP (1982) Stress amplification in the upper crust and the development of normal faulting. *Tectonophysics* 83:121–130
- Nakamura K (1977) Volcanoes as possible indicators of tectonic stress orientation: Principle and proposal. *J Volcanol Geotherm Res* 2:1–16
- Norini G, Capra L, Groppelli G, Lagmay AMF (2008) Quaternary sector collapses of Nevado de Toluca volcano (Mexico) governed by regional tectonics and volcanic evolution. *Geosphere* 4(5):854–871
- Norini G, Capra L, Groppelli G, Agliardi F, Pola A, Cortes A (2010) Structural architecture of the Colima Volcanic Complex. *J Geophys Res* 115(B12209):1–20. doi:10.1029/2010JB007649
- Norini G, Baez W, Becchio R, Viramonte J, Giordano G, Arnosio M, Pinton A, Groppelli G (2013) The Calama-Olacapato-El Toro fault system in the Puna Plateau, Central Andes: geodynamic implications and stratovolcanoes emplacement. *Tectonophysics* 608:1280–1297
- Nostro C, Stein RS, Cocco M, Belardinelli ME, Marzocchi W (1998) Two-way coupling between Vesuvius eruptions and southern Apennine earthquakes, Italy, by elastic stress transfer. *J Geophys Res* 103:24487–24504
- Okada Y (1992) Internal deformation due to shear and tensile faults in a half-space. *Bull Seismol Soc Am* 82:1018–1040
- Okal EA (2005) A re-evaluation of the great Aleutian and Chilean earthquakes of 1906 August 17. *Geophys J Int* 161:268–282
- Piersanti A, Spada G, Sabadini R, Bonafede M (1995) Global postseismic deformation. *Geophys J Int* 120:544–566
- Piersanti A, Spada G, Sabadini R (1997) Global postseismic rebound of a viscoelastic Earth: Theory for finite faults and application to the 1964 Alaska earthquake. *J Geophys Res* 102:477–492
- Pollitz FF, Bürgmann R, Romanowicz B (1998) Viscosity of oceanic asthenosphere inferred from remote triggering of earthquakes. *Science* 280:1245–1249

- Potent S, Reuther CD (2001) Neogene Deformationsprozesse im aktiven magmatischen Bogen Südcentralchiles zwischen 37° und 39 °S. Mitteilungen aus dem Geologisch-Palaontologischen Institut der Universität Hamburg 85:1–2
- Radic JP, Rojas L, Carpinelli A, Zurita E (2002) Evolución tectónica de la cuenca terciaria de Cura-Mallín, región cordillerana chileno argentina (36°30′-39°00′S). XV Congreso Geológico Argentino, Calafate, Argentina 3:233–237
- Rojas Vera E, Folguera A, Spagnuolo M, Gimenez M, Ruiz F, Martínez P, Ramos VR (2009) La neotectónica del arco volcánico a la latitud del volcán Copahue (38 °S), Andes de Neuquén. *Rev Asoc Geol Arg* 65(1):204–214
- Rojas Vera EA, Folguera A, Valcarce GZ, Bottesi G, Ramos VR (2014) Structure and development of the andean system between 36° and 39°S. *J Geodyn* 73:34–52
- Rosenau M (2004) Tectonics of the southern Andean intra-arc zone (38°–42°S). Ph.D. thesis, Free University, Berlin, Germany, pp 159
- Rosenau M, Melnick D, Echtler H (2006) Kinematic constraints on intra-arc shear and strain partitioning in the Southern Andes between 38°S and 42°S latitude. *Tectonics* 25:TC4013
- Sumita I, Manga M (2008) Suspension rheology under oscillatory shear and its geophysical implications. *Earth Planet Sci Lett* 269:468–477
- Tibaldi A (1995) Morphology of pyroclastic cones and tectonics. *J Geophys Res* 100(B12):24521–24535
- Toda S, Stein RS, Richards-Dinger K, Bozkurt S (2005) Forecasting the evolution of seismicity in southern California: animations built on earthquake stress transfer. *J Geophys Res* B05S16
- Toda S, Stein RS, Lin J, Sevilgen K (2011) Coulomb 3.3 User Guide
- Tormey DR, Hickey-Vargas R, Frey FA, López-Escobar L (1991) Recent lavas from the Andean volcanic front (33–42 °S); interpretations of along-arc compositional features. In: Harmon RS, Rapela CW (eds), *Andean Magmatism and its Tectonic Setting*. *Geol Soc Am* 265:57–77
- Varekamp JC, Ouimette AP, Herman SW, Bermudez A, Delpino D (2001) Hydrothermal element fluxes from Copahue, Argentina: a “beehive” volcano in turmoil. *Geology* 29:1059–1062
- Velez ML, Euillades P, Caselli A, Blanco M, Díaz JM (2011) Deformation of Copahue volcano: inversion of InSAR data using a genetic algorithm. *J Volcanol Geotherm Res* 202:117–126
- Walter TR (2007) How a tectonic earthquake may awake silent volcanoes: Stress triggering during the 1996 earthquake-eruption sequence at the Karymsky Volcanic Group, Kamchatka. *Earth Planet Sci Lett* 264(3–4):347–359
- Walter TR, Schmincke H-U (2002) Rifting, recurrent landsliding and Miocene structural reorganization on NW-Tenerife (Canary Islands). *Int J Earth Sci* 91:615–628
- Walter TR, Amelung F (2006) Volcano-earthquake interaction at Mauna Loa volcano, Hawaii. *J Geophys Res* 111:B05204
- Walter TR, Amelung F (2007) Volcanic eruptions following $M \geq 9$ megathrust earthquakes: implications for the Sumatra-Andaman volcanoes. *Geology* 35:539–542
- Wells DL, Coppersmith KJ (1994) New empirical relationships among magnitude, rupture length, rupture width, rupture area, and surface displacement. *Bull Seismol Soc Am* 84:974–1002
- Watt SFL, Pyle DM, Mather TA (2009) The influence of great earthquakes on volcanic eruption rate along the Chilean subduction zone. *Earth Planet Sci Lett* 277:399–407



<http://www.springer.com/978-3-662-48004-5>

Copahue Volcano

Tassi, F.; Vaselli, O.; Caselli, A.T. (Eds.)

2016, XII, 293 p. 172 illus., 130 illus. in color.,

Hardcover

ISBN: 978-3-662-48004-5